MECHTA
International Journal Of Mechanical Engineering Technologies & Applications
V06 N.1
ISSN 2722-3213 articles 2, pp. 11 – 24, 2025

FLUID FLOW CHARACTERISTICS IN A SHELL AND TUBE HEAT EXCHANGER WITH SWIRL BAFFLES

Aulia Rahman [1)] ✉ , Winarto [1)], Eko Siswanto [1)], Lilis Yulianti [1)], Rizky Kusumastuti [2)]

[1)] **Mechanical Engineering Department**
Brawijaya University
MT. Haryono, 167
Malang, Jawa-Timur, INDONESIA
auliarahman.fzn@gmail.com

[2)] **Graduate Institute of Energy Engineering**
National Central University
No. 300, Zhongda Rd, Zhongli District,
Taoyuan City, Taiwan

Abstract

This paper presents a numerical investigation into the fluid flow and heat transfer characteristics of a shell and tube heat exchanger (STHeX) equipped with baffles that induces swirl flow. A Computational Fluid Dynamics (CFD) model was developed to simulate the behavior of the STHeX, and its accuracy and reliability were verified by comparing the results with calculations obtained using the Bell-Delaware method. The two sets of calculations exhibited good agreement, validating the CFD model. The velocity component of the fluid flow was analyzed both qualitatively and quantitatively. The flow patterns of eddies on the shell-side of the STHeX were carefully examined and their correlation with thermal performance was investigated. This study demonstrates that the swirl flow baffle geometry leads to a more turbulent flow pattern, resulting in an increase in the overall heat transfer coefficient. The findings indicate that the swirl flow baffle enhances heat transfer performance and reduces pressure drop in comparison to a conventional STHeX.

Keywords: *Baffle Geometry, Numerical Simulation, Heat Exchanger, Velocity Components, Fluid Flow.*

1. INTRODUCTION

The shell and tube heat exchanger (STHeX) is extensively utilized in diverse industries owing to its uncomplicated processing, convenient maintenance, and versatile usability [1]. It assumes a pivotal function in energy conversion systems, encompassing power generation, chemical engineering, and the recuperation of waste heat [2]. STHeXs, which are commonly referred to as Super Thermoplastic High-pressure Exchangers, have gained recognition in various industries due to their exceptional ability to withstand high pressures, their straightforward manufacturing process, and their relatively affordable price point. Consequently, these desirable characteristics have rendered STHeX a widely favored option in the realm of industrial applications [3]. They possess the ability to endure elevated temperatures and pressures, rendering them appropriate for a diverse array of applications [4]. The utilization of STHeXs that incorporate various configurations of baffles has been the subject of investigation in order to augment the efficiency of heat transfer and enhance overall performance [5].

Understanding the characteristics of fluid flow in heat exchangers is crucial for analyzing and optimizing their performance, as researchers can identify areas for improvement and design more efficient heat exchangers by studying parameters like velocity, pressure, and temperature. The fluid film that flows around a surface is influenced

Corresponding Author:
✉ **Aulia Rahman**
auliarahman.fzn@gmail.com
Received on: 2024-03-20
Revised on: 2024-06-19
Accepted on: 2024-06-24

DOI: 10.21776/MECHTA.2025.006.01.2

by various geometrical shapes. The alteration of this flow film has a direct impact on the mechanism responsible for the rate of heat transfer [6]. The subsequent step in this procedure involves implementing it to STHeX, in which the modification of the baffle's structure is carried out. By modifying the configuration of the baffle, a unique flow pattern of fluid is obtained [7], [8], [9]. Helical baffles, such as those found in heat exchangers, induce a spiral flow pattern that serves to enhance the heat transfer coefficient. This is achieved through the amplification of the radial velocity gradient and the reduction of the boundary layer thickness, thus effectively mitigating stagnation areas within the flow [10]. The flow behavior and thermal exchange within a heat exchanger with helical baffles can be influenced by various factors, including the angle of the helix [11][12]. An analysis of the helical baffle and the conventional segmented baffle demonstrated a noticeable increase in the rate of heat transfer by 5.6%, accompanied by a corresponding reduction in pressure drop by 13% [11]. Subsequently, as a result of refining the configuration of the helix baffle, it was documented that there was a notable augmentation of 28.3% in the heat transfer coefficient, concomitant with a corresponding pressure drop of 19.37% [13]. In addition to helical baffles, many studies have also been conducted with other baffle shapes. Furthermore, three curved baffle arrangements were investigated. By utilizing a novel configuration of curved baffles in the heat exchanger, the transfer of heat between two fluids is enhanced due to improved mixing of the colder fluid. This results in the generation of turbulence, which in turn promotes greater contact between the cold fluid and the hot pipe surface, thereby facilitating superior heat transfer. The most effective baffle design increases the efficiency of the heat exchanger by 51.31% and concurrently reduces energy loss resulting from pressure drop by approximately 12% [14]. In another study, it was learnt that the use of triangular ribbed tubes with disc baffles increased the heat transfer by 39% compared to conventional STHE. The stagnation area formed in the new design has decreased. This helps more fluids to be actively involved in heat transfer, so that the heat exchanger performs better overall [8]. Another study has reported that baffles can also contribute to the fragmentation of slow-moving areas within the fluid, consequently leading to an enhancement in the overall effectiveness of the heat transfer process [15]. Several STHeX studies have reported twisted fluid flow resulting from trapezoidal baffle. The enhancement of the twisted flow manifests in the form of an augmented heat transfer coefficient and pressure drop [16]. This is primarily due to the rotational motion of the fluid, which incessantly alters its direction, thereby effectively disrupting the formation of stagnant fluid layers. The resulting disruption mitigates the occurrence of 'hot spots' or regions where the fluid is inadequately cooled, culminating in a more uniform temperature distribution [17]. Furthermore, the continuous mixing of the fluid engendered by the swirling flow ensures that colder fluid is consistently brought into contact with heated surfaces, thereby improving the overall heat transfer process [18]. The conventional form of the STHeX design is altered to create a twisted flow, achieved by examining the impact of the baffle cut on the rotated segmented baffle [19]. By adjusting the inclination and separation of these baffles, the unique configuration is able to control the serpentine fluid motion, transforming it into a swirling movement, which in turn enhances the efficiency of heat transfer as compared to the linear flow observed in previous designs. Consequently, this capability can yield improved heat transfer performance without necessitating excessive fluid propulsion, thus leading to energy conservation.

When analyzing the characteristics of fluid flow dynamics in heat exchangers, computational fluid dynamics (CFD) can be utilized to characterize the flow and transfer of heat [20]. These calculations involve solving the governing equations of continuity, momentum, and energy conservation through numerical techniques like the finite volume method [21]. Through these simulations, valuable insights can be gained regarding the patterns of flow, velocity profiles, and temperature distribution within a system [22]. Moreover, CFD

simulations can assist in predicting heat transfer coefficients and evaluating the performance of heat exchangers. The results obtained from these simulations can be utilized to optimize the design of heat exchangers and enhance their efficiency [23].

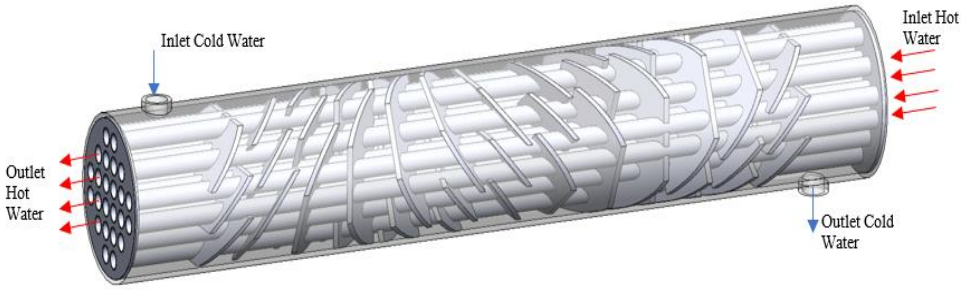

Fig. 1 Geometry of computational STHeX

The main goal of this research endeavor is to thoroughly analyze and examine the fluid flow properties of the unique STHeX baffle, thereby establishing its correlation with the enhanced performance of STHeX in terms of heat transfer and pressure drop. The STHeX swirl baffle was subjected to a comprehensive investigation utilizing the methodology of Computational Fluid Dynamics (CFD) in a numerical study. In order to ascertain the validity and reliability of the obtained results, a traditional heat exchanger was subjected to rigorous testing, with the results being compared to the mathematical calculations from existing literature. The outcomes derived from the CFD analysis were subsequently juxtaposed with the aforementioned mathematical calculations, thereby facilitating the identification of a compelling correlation between the measured and simulated results. It is important to note that this study serves to underscore the fact that the shell and tube heat exchanger, featuring the novel baffle design, possesses distinctive fluid flow characteristics when compared to the conventional STHeX.

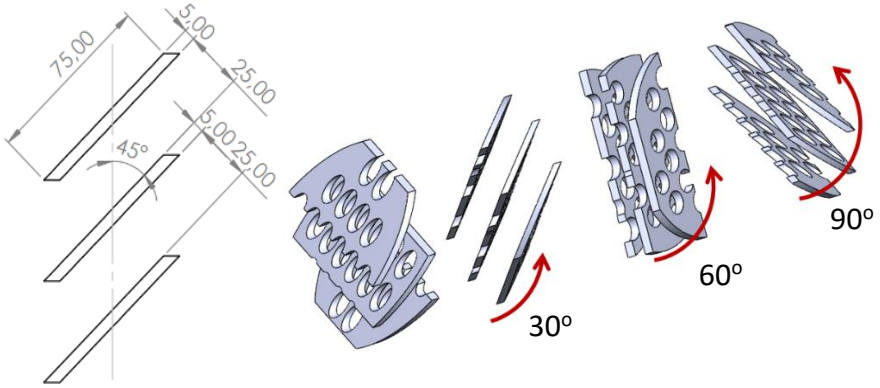

Fig. 2: The geometric properties of a baffling structure.

2. MATERIALS AND METHODS

2.1. Geometry of the model

The heat exchanger in the physical model is equipped with a baffle arrangement consisting of inclined plates that are twisted at specific angles. The computational analysis utilizes a

geometry model, as depicted in Figure 1. The specific dimensions of the geometric details can be found in Table 1. In a comprehensive and thorough manner, the configuration of the baffles is depicted and exemplified by the visual representation provided in Figure 2. It is crucial to note that each individual baffle has undergone a rotation of precisely 30 degrees on every single bundle of baffles.

Tabel 1. Geometric Detail Dimension S

Parameters	**Size/Qty**
Inner diameter of the shell (mm)	160
The length of the tube (mm)	1034
The diameter of the tube (mm)	19
Tube spacing (mm)	23.81
The arrangement of tubes	Quadratic
Baffle thickness (mm)	4
The interval between baffles (mm)	64

2.2. Scheme of the turbulence and the governing equation

In computational modeling, it is imperative to satisfy the governing equation, which consists of the subsequent equations [21]:

Continuity equation:

$$\frac{\partial \rho}{\partial t} + \nabla(\rho u) = 0 \quad (1)$$

Momentum equation:

$$\frac{\partial(\rho u)}{\partial t} + \nabla(\rho u \mathbf{u}) = -\frac{\partial p}{\partial x} + \nabla(\mu \, grad \, u) + S_{Mx} \quad (2)$$

$$\frac{\partial(\rho v)}{\partial t} + \nabla(\rho v \mathbf{u}) = -\frac{\partial p}{\partial y} + \nabla(\mu \, grad \, v) + S_{My} \quad (3)$$

$$\frac{\partial(\rho w)}{\partial t} + \nabla(\rho w \mathbf{u}) = -\frac{\partial p}{\partial z} + \nabla(\mu \, grad \, w) + S_{Mz} \quad (4)$$

Energy equation:

$$\frac{\partial(\rho i)}{\partial t} + \nabla(\rho i \mathbf{u}) = -p \, \nabla \boldsymbol{u} + \nabla(k \, grad \, T) + \Phi + S_i \quad (5)$$

Due to the intricate nature of fluid flow on the shell side, the choice of turbulence models necessitates a certain level of precision in calculating the trajectories of the flow with a higher degree of curvature. A study conducted by Liu *et al.*[24] confirmed that among the various turbulence models, RNG k-ε exhibits a superior level of accuracy. As a result, RNG k-ε has been opted for as the turbulence model in the present investigation. The enhanced wall function was employed in order to effectively address the fluid motion in the immediate.

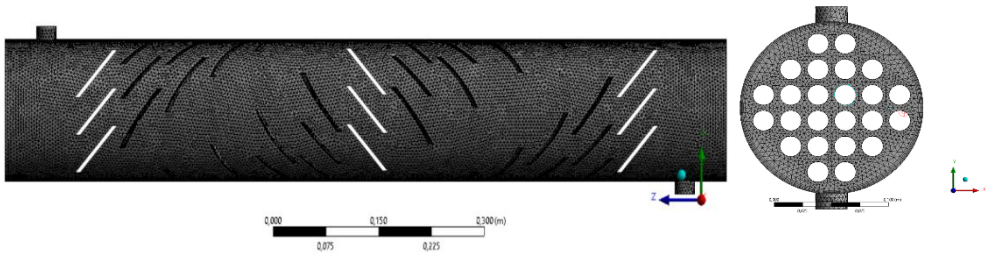

Fig. 3. Mesh structure for the computation.

vicinity of the wall. In order to accurately capture the various aspects of the flow, such as energy, momentum, pressure, turbulent kinetic energy, and turbulent dissipation rate, the first-order upwind method was implemented. This approach ensured that all relevant variables and phenomena were adequately accounted for and accounted for in a comprehensive manner.

2.3. The boundaries and fundamental assumptions.

Water is used as the operating medium for both shell and tube sides, effectively facilitating the heat transfer process inside the heat exchanger. Careful determination of the mass flow rate was carried out at the inlets of both sides, ensuring accurate measurements for subsequent analyses. To create a controlled experimental environment, the temperature was set at 50^{o} C for the tube side and 28^{o} C for the shell side, allowing the examination of heat transfer phenomena under specific thermal conditions. In this study, it was assumed that the turbulent flow would remain stable for the duration of the experiment, thus providing consistent and reliable results. In addition, it was also assumed that the physical properties of the working medium would remain constant, thus eliminating potential variations that could affect the results. To simplify the geometry of the shell-and-tube heat exchanger (STHeX), the distance between the baffle and the tubes was deliberately neglected, thus allowing for a more straightforward and concise analysis.

2.4. Grid independence

Due to the intricacy inherent in the geometric characteristics observed in STHeX, which is characterized by the presence of baffled inclined vortices, a technologically adaptive approach was employed in order to enhance the precision and reliability of the mesh structures. This approach specifically entailed the utilization of tetrahedral and pyramidal structureless meshes as a means to improve the overall accuracy of the mesh structures. In order to elucidate and illustrate this innovative technique, the mesh specific to STHeX was exemplified and visually represented in the form of Figure 3. Subsequently, an analysis of the geometric attributes was conducted with the aim of determining the state of mesh independence, which was then simulated at a predetermined mass flow rate of 0.3010 kg/s. The results obtained from this simulation were effectively presented and showcased in Figure 4, wherein it can be clearly discerned and observed that there exists a direct correlation between the number of cells employed within the mesh and the overall heat transfer coefficient value. This notable observation serves to underscore and demonstrate that an increased number of cells utilized in the numerical calculation significantly contributes to a higher degree of accuracy. Consequently, it can be deduced that a more comprehensive numerical calculation necessitates a higher computational cost due to the increased complexity and intricacy involved in the calculations [25].

From the analysis presented in Figure 4, it is readily apparent that the relative difference in heat transfer coefficient is negligible, less than 1%, when comparing a cell count of 5.49 million to 6.14 million. This observation implies that the variation in heat transfer coefficient between these two cell counts is of minimal significance. It is also worth noting that the values of the total heat transfer coefficient, denoted by U, as well as the pressure drop, are consistently below the average value at any given point. This means that a grid-independent solution has been achieved, where the numerical simulation is not affected by the grid size. In order to ensure computational efficiency and accuracy, a grid system of 5.49 million cells was chosen as this was considered sufficient for accurate results. The decision to use this particular number of cells was made after careful consideration of factors such as computational efficiency and accuracy of results. It is important to note that similar solutions

have been explored and used in other model cases, demonstrating the applicability and validity of this approach to different scenarios in the field. The use of comparable grid systems has been explored and established in previous studies, further underlining the soundness of this choice in the present investigation.

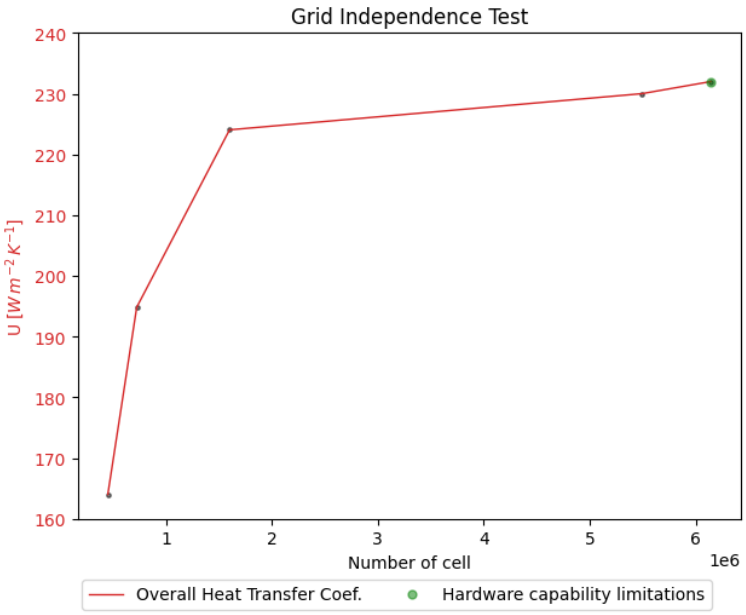

Fig. 4. Comparison of the heat transfer coefficient across various grid numbers.

2.5. Validation of numerical simulation

The validation of the accuracy and efficiency of the numerical method is conducted through a comparison study with simulation results, whereby mathematical calculations employing the bell-Delaware method are utilized [26]. This approach serves as a means to assess the reliability and effectiveness of the numerical technique, thereby ensuring the veracity and efficiency of the computations. The determination of the heat transfer coefficient is accomplished through the utilization of equations (7)-(16), which have been formulated based on previous investigations [5], [27], [28].

$$\Delta T_1 = T_{h,i} - T_{c,o} \tag{7}$$

$$\Delta T_2 = T_{h,o} - T_{c,i} \tag{8}$$

$$\Delta T_{lmtd} = \frac{\Delta T_1 - \Delta T_2}{ln(\Delta T_1/\Delta T_2)} \tag{9}$$

$$A = N_t \pi d l \tag{10}$$

$$Nu_t = 1.86 \left(\frac{G_s d_i}{\mu_i} \frac{\mu_t C_t}{k_t} \frac{d}{L}\right)^{0.33} \left(\frac{\mu_b}{\mu_w}\right)^{0.152} \tag{11}$$

$$h_t = \frac{Nu_t\, k}{d_i} \tag{12}$$

$$Nu_s = 0.36 \left(\left(\frac{G_s d_i}{\mu_i}\right)^{0.55}\right) \left(\left(\frac{\mu_s C_s}{k_s}\right)^{0.33}\right) \left(\frac{\mu_b}{\mu_w}\right)^{0.14} \tag{13}$$

$$h_o = \frac{Nu_s\, k}{d_i} \tag{14}$$

The heat transfer surface area, denoted by the symbol A, is determined by the number of tubes installed (Nt), the tube diameter (d), and the tube length (l). The logarithmic mean temperature difference (Tlmtd) is represented by the symbol Tlmtd. The calculation of the Nusselt number (Nu) is performed separately on both the shell side and the tube side. These calculations take into consideration the different flow patterns that occur, with laminar forced convection being applied on the tube side and turbulent forced convection on the shell side. It is worth noting that the Reynolds number (Re) and the Prandtl number (Pr) are calculated using the same formula on both the shell side and the tube side.

$$h_s = h_o J_c J_i J_s J_b J_r \tag{15}$$

The Bell-Delaware method, a renowned calculation method in the field of STHeX, comprehensively considers flow losses in heat transfer [29]. This method is highly acclaimed and carefully examines the relationship between flow losses and heat transfer efficiency [30]. By including flow losses in its calculations, the Bell-Delaware method provides a more accurate representation of heat transfer in STHeX systems [31]. Through its rigorous analysis and incorporation of flow losses, this method contributes to the advancement of knowledge in heat transfer calculations [11]. The representation of the losses in flow is denoted by the variables Jc, Ji, Js, Jb, and Jr. In order to improve the correlation specifically on the shell side, these losses are subsequently multiplied by the heat coefficient. The heat coefficient serves as an enhancement factor, which amplifies the impact of the losses in flow, thereby aiding in the enhancement of the correlation on the shell side [32]. The detailed breakdown of the factors and variables involved in quantifying flow loss within a system can be found in table 2, which provides a comprehensive explanation of the flow loss notation.

The expression for the overall heat transfer coefficient on the shell side, denoted as U, can be determined.

$$U = \frac{1}{\left(\frac{d_o}{d_i}\frac{1}{h_t}\right)+\left(\frac{d_o ln(d_o/d_i)}{2k}\right)+\left(\frac{1}{h_s}\right)} \tag{16}$$

The symbol di is employed to indicate the internal diameter of the tube, wherein di signifies the measurement of the innermost portion of the tube. Then, the variable k is utilized to denote the thermal conductivity of the tube wall, which represents the capacity of the material.

Tabel. 2. The variables used in bell-Delaware method.

Item	Description
J_c	The window effect of each baffle piece is depicted by the aforementioned.
J_i	The leakage effect between the shell and baffle, as well as between the tube and baffle, is represented by this parameter.
J_r	The flow effect between the inner shell wall and tube bundle, as well as the partition pass effect, are represented in this study.
J_b	The flow effect between the inner shell wall and tube bundle, as well as the partition pass effect, is represented by the aforementioned.
J_s	The impact of uneven spacing of the inlet or outlet baffles, which deviates from the central baffle spacing, is being depicted.

composing the tube wall to conduct heat. Furthermore, hs is employed to characterize the heat transfer coefficient on the shell side, which signifies the efficiency of heat transfer between the shell and the fluid flowing through it. Lastly, ht is utilized to represent the heat

transfer coefficient on the tube side, which quantifies the degree to which heat is transferred between the fluid within the tube and the tube wall. U factors are defined as follows [33],[34]:

$$\varepsilon = \frac{C_c(T_{c2}-T_{c1})}{C_{min}(T_{h1}-T_{c1})} \quad (17)$$

$$Q = \varepsilon\left(\dot{m}c_p\right)_{min}(T_{h1} - T_{c1}) \quad (18)$$

$$U = \frac{Q}{AF\Delta T_{lmtd}} \quad (19)$$

$$Q = \left(\dot{m}c_p\right)_h(T_{h1} - T_{h2}) = \left(\dot{m}c_p\right)_c(T_{c2} - T_{c1}) \quad (20)$$

Numerical data calculation yields temperature data for each fluid flow outlet, providing valuable information about the thermal behavior of the system. By analyzing the temperature data obtained at the outlet, one can proceed to compute the overall heat transfer coefficient utilizing the equations 17-19, which describe the relationship between temperature and heat transfer. Comparing this calculated value with the heat transfer coefficient obtained from mathematical calculations allows for a comprehensive assessment of the system's thermal performance.

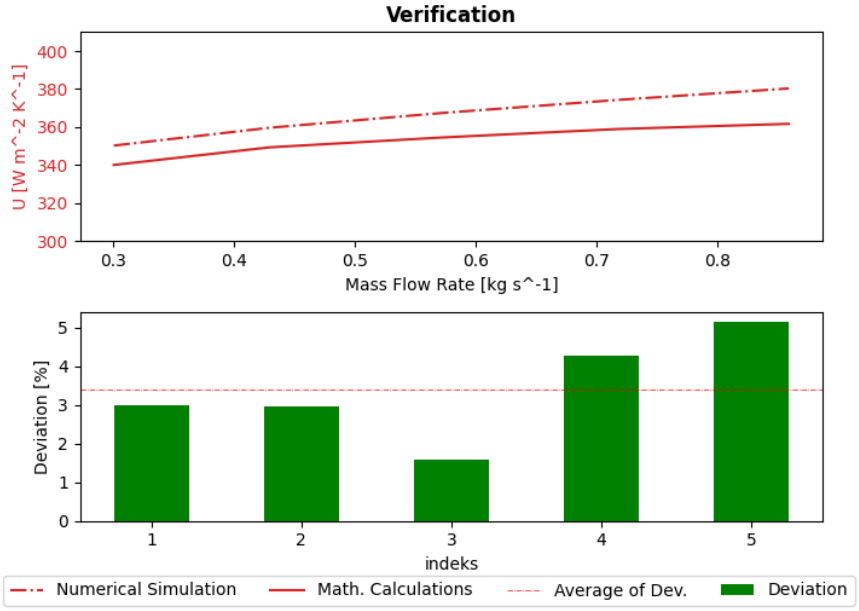

Fig. 5. Verification between numerical simulation and Bell-Delaware Method

The computation outcomes are obtained using the equations mentioned above. Deviation analysis allows for a quantitative evaluation of the agreement between the simulation results and those obtained from mathematical calculations. Visual aids such as Figure 5 and graphs can also assist in interpreting the results of the deviation analysis. By comparing the simulated and mathematical calculations, it is possible to identify patterns or trends of deviation, gaining insight into the behavior of the numerical model. Additionally, sensitivity analysis can be performed to assess the influence of input variables on simulation outcomes and investigate the extent to which changes in these variables affect discrepancies. This text appears to already meet the desired characteristics. No changes have been made [35]. Figure 5 illustrates that the mean discrepancy between the calculation base on bell-Delaware method and computational representation is 3.51%, accompanied by a 4.01% discrepancy in the

decline of pressure. Next, the energy balance analysis is calculated with equation 20. Then the value of Q hot water and Q cold water is obtained in the same value. These figures fall within a rational spectrum and lend credence to the trustworthiness of the numerical simulations.

3. RESULTS

Fluid flow velocity at the inlet shell produces mass flow rates of 0.301025 kg/s, 0.429801 kg/s, 0.600524 kg/s, 0.676239 kg/s, 0.859418 kg/s for STHeX Inclined Segmental Baffle respectively. Meanwhile, the mass flow rate on the tube side is constant at 0.1211 kg/s. Simulation results using AN-SYS show that the flow in STHeX forms a helical flow. As seen in Figure. 4, it can be seen that the fluid flow follows the shape of the baffle which has a slope angle at each baffle arrangement. The helical flow has a speed of about 0.81 m/s to 2.38 m/s, this value is much higher than the average flow that passes through the tube arrangement, but this is good for reducing the pressure drop on the shell side. The average speed of cold-water fluid washing the pipe is 0.025 m/s, 0.039 m/s, 0.058 m/s, 0.072 m/s, and 0.0891346 m/s respectively at different mass flow rates. The fluid flow speed is directly proportional to the heat transfer coefficient as seen in Figure. 3.

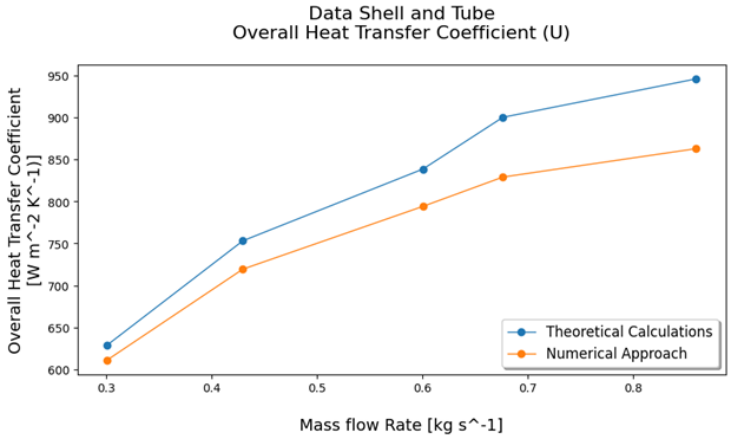

Figure 3. Comparison of simulation results and theoretical calculations for STHeX segmented baffle.

The heat transfer coefficient in Figure. 3 compares theoretical calculations with numerical simulations. The average deviation value between these two values is 5.8%. The highest deviation occurs at the highest mass flow rate, this is because there is a need to adjust the grid for each additional speed value. The simulation cost is directly proportional to the number of meshes, this is because a more detailed simulation will require more adequate hardware.

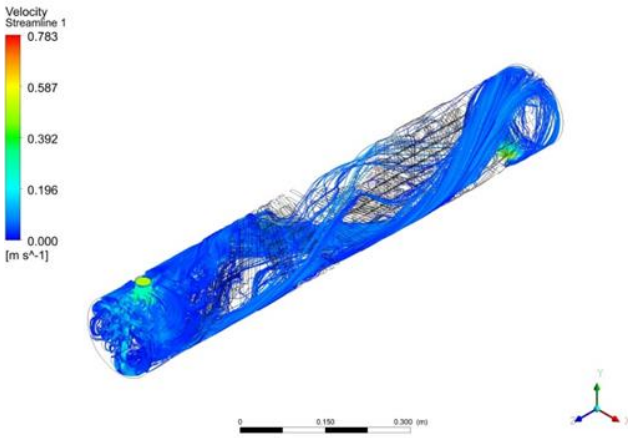

Figure 4. Streamline cold water fluid on shell side

4. DISCUSSION

Then, to see the flow characteristics, you need to look in more detail at the plan for each baffle. As seen in Figure. 5 that the longitudinal flow velocity in the z-axis direction is found in the top gap of the baffle to the shell surface and the gap below the baffle to the shell surface. Every change in angle in the baffle arrangement changes the direction of flow so that the flow in the gap is not uniform. This non-uniformity is caused by the empty gap between each baffle arrangement and the next baffle arrangement. On the middle side of the tube arrangement, the speed tends to be lower because the baffle arrangement blocks fluid flow in that section.

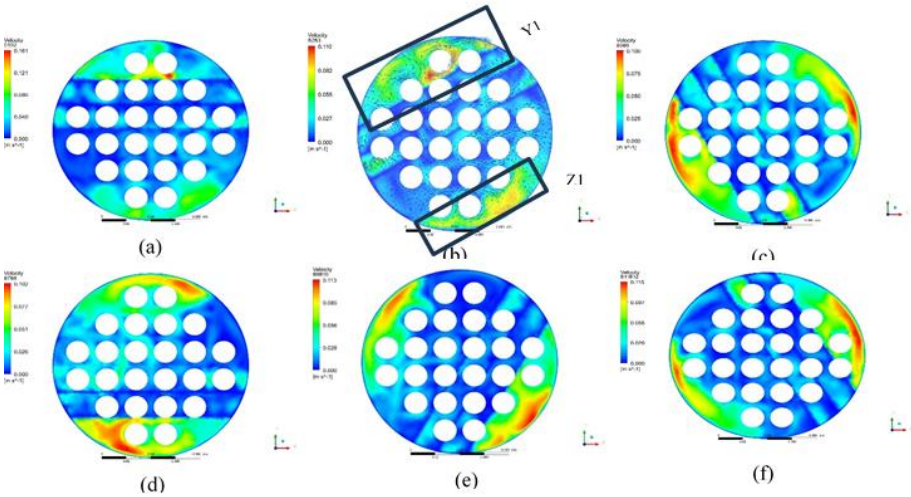

Figure 5. Velocity contours between baffles, (a) first and second baffles, (b) third and fourth baffles, (c) fifth and sixth baffles, (d) seventh and eighth baffles, (e) ninth and tenth baffles and (f) baffles eleventh and twelfth

The velocity vector in Figure 5 (b) shows that the direction of fluid flow only washes one tube in area Y1 and two tubes in area Z1 so that the heat transfer in these two tubes has a fairly high thermal coefficient. This is because the higher the speed, the higher the Reynolds value and the resulting coefficient is greater than on other tubes. As can be seen in Figure 8 (b), the temperature of the cold air fluid increases in the section with the flow velocity in the

middle section. The high velocity of fluid flow in the longitudinal flow direction makes the movement of heat tend to be smaller.

Pressure drop on STHeX Inclined Segmental Baffles is depicted in Figure. 6. Where the highest pressure is in areas Y_2 and Z_2 where the baffle is tilted. Meanwhile, parts that have low pressure are a form of pressure drop caused by the presence of baffles. Each baffle has different pressure losses due to the increase in angle in each baffle arrangement.

Pressure drop is a factor that greatly influences the operation of a STHeX [16]. This is because the greater the pressure drop in STHeX, the additional energy required to flow the fluid to reach the desired pressure in the next process. Some STHeX applications in industrial installations involve several levels of SHTeX. Pressure drops at STHeX in multilevel installations will result in significant energy losses.

Another parameter to see the reliability of STHeX is to look at the overall summer growth coefficient. The overall heat transfer coefficient (U) is how much heat energy is transferred from one fluid to another fluid. The correlation between U and pressure drop (ΔP) can be seen in Figure 7 which com-pares U/ΔP on conventional STHeX segmented baffles with STHeX Inclined Segmental Baffles.

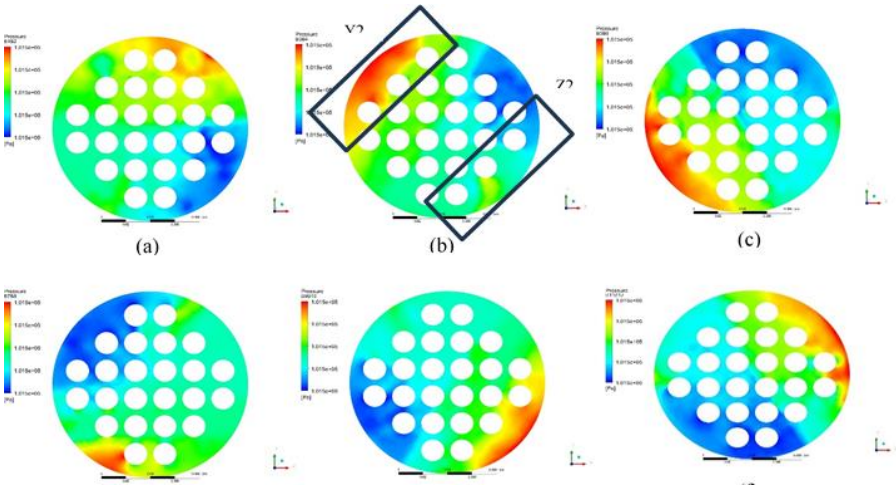

Figure 6. Pressure contours between baffles (a) first and second baffles, (b) third and fourth baffles, (c) fifth and sixth baffles, (d) seventh and eighth baffles, (e) ninth and tenth baffles and (f) eleventh and twelfth

In Figure. 7 it can be seen that as the mass flow rate increases, the U/ΔP value decreases for each STHeX that is compared. This is because the values of U and ΔP are directly proportional to the mass flow rate of a STHeX. With increasing mass flow rate the difference between the two is quite constant, around 34.77%. At a mass flow rate of 0.85, the biggest difference between the two STHeX is 37.18%. Thus, the energy required on multilevel STHeX will be smaller on STHeX with Inclined Segmental Baffles compared to STHeX segmented baffles.

This phenomenon occurs because the fluid flow velocity in the STHeX segmented baffle which passes through the tube arrangement is higher than the fluid flow velocity in the STHeX with Inclined Segmental Baffles. As seen in Figure. 8 (c) at a speed of 0.858 is on a wider surface. Thus, the heat transfer coefficient in that area is quite high which results in lower heat transfer in that area, which can be seen in Figure. 8(c). On the other hand, the fluid flow that does not pass through the baffle arrangement has the same speed so that there is no heat transfer in that area according to the figure in Figure. 8(c).

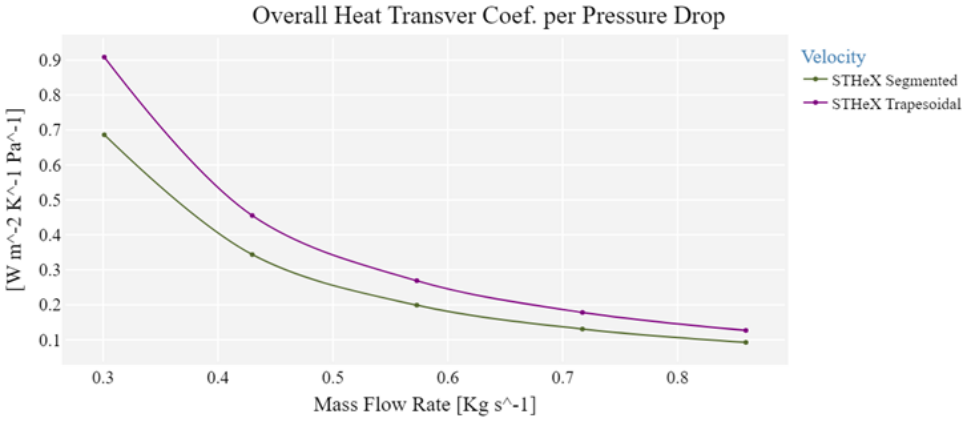

Figure 7. Overall coefficient heat transfer between conventional STHeX segmented baffle with STHeX Inclined Segmental Baffles

In Figure. 8 (a) The fluid flow flowing in the tube arrangement tends to be lower and the highest speed is only in the baffle gap area against the shell wall. Thus Figure. 8 (b) the heat transfer in the tube array is higher when compared to the STHeX segmented baffle Figure. 8 (c).

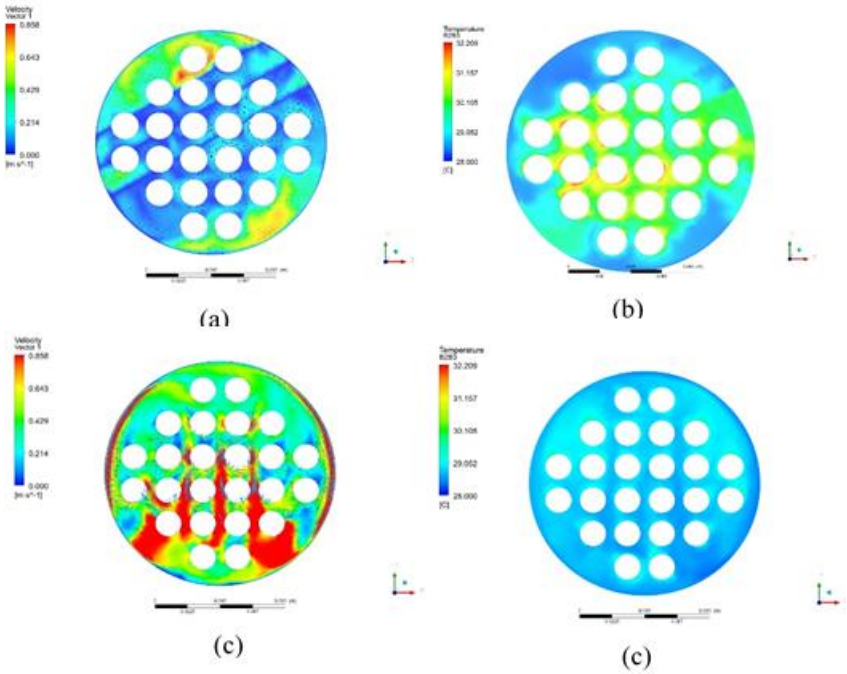

Figure 8. The difference between STHeX segmented baffle and STHeX Inclined Segmental Baffles in speed and temperature

After reviewing the temperature and heat transfer results, a review was carried out on the pressure drop between STHeX segmented baffles and STHeX Inclined Segmental Baffles. As seen in Figure. 9 that the pressure drop on the STHeX segmented baffle tends to be more constant with each additional baffle. This was also found in the different simulated mass flow rates. In contrast to STHeX Inclined Segmental Baffles, the phenomenon that forms with each additional baffle is quite fluctuating as the mass flow rate increases. This is

because the flow does not pass through the gap between the baffles, but the fluid flows through the gap between the baffle and the shell wall.

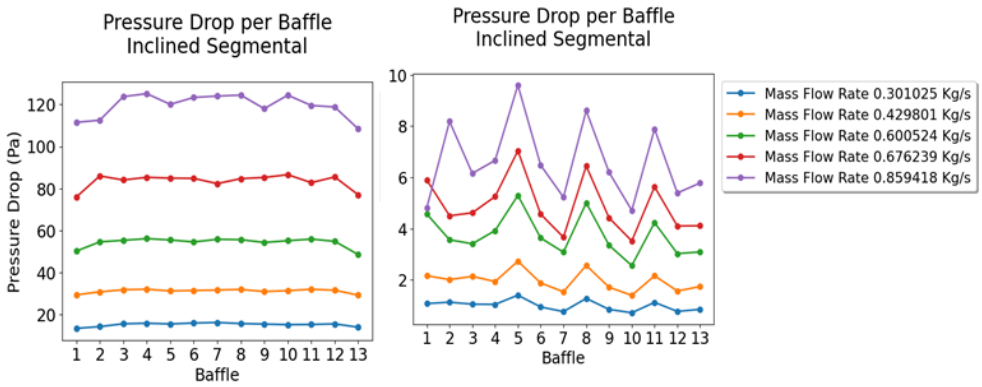

Figure 9. Pressure drop between conventional STHeX segmented baffle with STHeX Inclined Segmental Baffles

5. CONCLUSION

Shell and tube heat exchanger (STHeX) design development is ongoing in an effort to make the system more efficient. Investigating the best baffle design is one way to do this. Investigation of the new STHeX construction with inclined segment baffles was carried out. Three-dimensional modeling and numerical approaches of CFD software were used to conduct the experiments. The pressure drop value is greatly reduced compared to standard STHeX, but the heat transfer coefficient value is lower. Determination of the value of the total heat transfer coefficient per pressure loss (U/ΔP) is required. It is known that the average difference in U/ΔP values reaches 34.77% and the highest increase in value is 37.18% at a mass flow rate of 0.859 kg/s. Based on the results, STHeX with oblique segment partition improves.

REFERENCES

[1] R. V. Rao and A. Saroj, "Economic optimization of shell-and-tube heat exchanger using Jaya algorithm with maintenance consideration," Appl Therm Eng, vol. 116, pp. 473–487, 2017, doi: 10.1016/j.applthermaleng.2017.01.071.

[2] Z. H. Ayub, D. Yang, T. S. Khan, E. Al-Hajri, and A. H. Ayub, "Performance characteristics of a novel shell and tube heat exchanger with shell side interstitial twisted tapes for viscous fluids application," Appl Therm Eng, vol. 134, pp. 248–255, Apr. 2018, doi: 10.1016/j.applthermaleng.2018.01.054.

[3] X. Gu, W. Chen, Y. Fang, S. Song, C. Wang, and Y. Wang, "Analysis of flow dead zone in shell side of a heat exchanger with torsional flow in shell side," Appl Therm Eng, vol. 180, Nov. 2020, doi: 10.1016/j.applthermaleng.2020.115792.

[4] H. Kücük, M. Ünverdi, and M. Senan Yılmaz, "Experimental investigation of shell side heat transfer and pressure drop in a mini-channel shell and tube heat exchanger," Int J Heat Mass Transf, vol. 143, Nov. 2019, doi: 10.1016/j.ijheatmasstransfer.2019.118493.

[5] C. Yu, Z. Ren, and M. Zeng, "Numerical investigation of shell-side performance for shell and tube heat exchangers with two different clamping type anti-vibration baffles," Appl Therm Eng, vol. 133, pp. 125–136, Mar. 2018, doi: 10.1016/j.applthermaleng.2018.01.029.

[6] J. Ji, F. Li, B. Shi, and Q. Chen, "Analysis of the effect of baffles on vibration and heat transfer characteristics of elastic tube bundles," International Communications in Heat and Mass Transfer, vol. 136, Jul. 2022, doi: 10.1016/j.icheatmasstransfer.2022.106206.

[7] P. Stehlík, J. Němčanský, D. Kral, and L. W. Swanson, "Comparison of correction factors for shell-and-tube heat exchangers with segmental or helical baffles," Heat Transfer Engineering, vol. 15, no. 1, pp. 55–65, Jan. 1994, doi: 10.1080/01457639408939818.

[8] J. Wen, X. Gu, M. Wang, S. Wang, and J. Tu, "Numerical investigation on the multi-objective optimization of a shell-and-tube heat exchanger with helical baffles," International Communi-cations in Heat and Mass Transfer, vol. 89, pp. 91–97, Dec. 2017, doi: 10.1016/j.icheatmasstransfer.2017.09.014.

[9] H. Sasongko, H. Mirmanto, G. Bangga, E. F. Nugrahani, and J. N. Pasaribu, "Numerical approach of the blade shape and number on the performance of multiple blade closed type impulse wind turbine," International Journal of Mechanical Engineering Technologies and Applications, vol. 4, no. 2, pp. 220–235, Jun. 2023, doi: 10.21776/mechta.2023.004.02.11.

[10] X. Gu, Y. Luo, X. Xiong, K. Wang, and Y. Wang, "Numerical and experimental investigation of the heat exchanger with trapezoidal baffle," Int J Heat Mass Transf, vol. 127, pp. 598–606, Dec. 2018, doi: 10.1016/j.ijheatmasstransfer.2018.07.045.

[11] J. Wen, H. Yang, S. Wang, S. Xu, Y. Xue, and H. Tuo, "Numerical investigation on baffle con-figuration improvement of the heat exchanger with helical baffles," Energy Convers Manag, vol. 89, pp. 438–448, Jan. 2015, doi: 10.1016/j.enconman.2014.09.059.

[12] A. A. Abbasian Arani and R. Moradi, "Shell and tube heat exchanger optimization using new baffle and tube configuration," Appl Therm Eng, vol. 157, Jul. 2019, doi: 10.1016/j.applthermaleng.2019.113736.

[13] D. E. Wahyudi, S. Nur'aini, W. K. Dewi, R. M. Aisyah, and E. L. Septiani, "The Calculation of Expense Reduction based on the Efficiency of Cyclone by Computational Fluid Dynamic," In-ternational Journal of Mechanical Engineering Technologies and Applications, vol. 2, no. 2, p. 85, Jul. 2021, doi: 10.21776/mechta.2021.002.02.1.

[14] C. Ranganayakulu and K. N. Seetharamu, "Compact Heat Exchangers – Analysis, Design and Optimization using FEM and CFD Approach," 2018.

[15] R. W. Serth, "Process Heat Transfer," Kingsville, Texas, USA, 2007.

[16] Y. Lei, Y. Li, S. Jing, C. Song, Y. Lyu, and F. Wang, "Design and performance analysis of the novel shell-and-tube heat exchangers with louver baffles," Appl Therm Eng, vol. 125, pp. 870–879, 2017, doi: 10.1016/j.applthermaleng.2017.07.081.